Characterizing *slc8a4b* as an Osteoblast Marker in *Danio rerio*

Olaf Baumeister Warren Holmes Corning

A thesis
submitted in partial fulfillment of the
requirements for the degree of

Master of Science in Bioengineering

University of Washington
2025

Committee:
Ronald Y. Kwon
Marta Scatena
Cole Trapnell

Program Authorized to Offer Degree:
Department of Bioengineering

University of Washington

ABSTRACT

Characterizing *slc8a4b* as an Osteoblast Marker in *Danio rerio*

Olaf Baumeister Warren Holmes Corning

Chair of the Supervisory Committee:
Ronald Y. Kwon
Department of Orthopaedic Surgery and Sports Medicine

The *solute carrier family 8 member 4b* (*slc8a4b)* is an emerging marker for osteoblasts in zebrafish, enabling further study of healthy bone development, bone regeneration, and skeletal diseases. To guide future use of *slc8a4b* as an osteoblast marker, this study aims to identify which osteoblast functions *slc8a4b* expression is most closely associated with, describe where in developing bone tissue *slc8a4b* is expressed, and demonstrate the utility of *slc8a4b* to demarcate cells poorly captured by other markers. The analysis of pre-existing single-cell RNA-sequencing (scRNA-seq) data showed osteoblasts expressing *slc8a4b* had similar transcriptional profiles as cells marked by other osteoblast markers but reduced expression of matrix synthesis genes. The spatial expression of *slc8a4b* in the 3 days post fertilization (dpf) opercle and cleithrum was visualized using Hybridization Chain Reaction RNA Fluorescence *in situ* hybridization (HCR RNA-FISH). These images revealed more centralized expression of *slc8a4b* compared to *runx2b* and *sp7* in the 3dpf opercle and compared to *runx2b* in the dorsal portion of the 3dpf cleithrum. HCR images of *tnfrsf11a* (RANK), recently identified as an important osteogenic regulator, showed substantial overlap in its spatial expression with *slc8a4b* suggesting *slc8a4b's* potential use in future studies of *tnfrsf11a*. The utility of *slc8a4b* as a marker was reinforced by the scRNA-seq data that showed the *slc8a4b* expression to be high and specific within osteoblasts, more osteoblasts expressing *slc8a4b* than any other non-collagen osteoblast marker, and substantial co-expression of *slc8a4b* in cells expressing other osteoblast markers. This specificity to osteoblasts, similarity and overlap with other markers, and large number of expressing cells, makes *slc8a4b* an excellent tool for future osteoblast research in zebrafish.

Introduction

Skeletal diseases, such as osteoporosis, have a substantial human cost. Osteoporosis, a reduction of bone mineral density and bone mass that increases the risk of fractures, has been reported at a global prevalence of 23.1% (95% CI 19.8–26.9) among women and at 11.7% (95% CI 9.6–14.1) among men of the world. (GBD 2019 Fracture Collaborators 2021). The annual direct costs of treating osteoporotic fractures in Canada, Europe, and the USA alone is estimated to be between 5 and 6.5 trillion USD (Rashki Kemmak et al. 2020).

Osteoblasts, or 'bone-forming cells', are mesenchymal cells that directly regulate bone matrix synthesis and mineralization and indirectly regulate bone resorption (Rosenberg, Rosenberg, and Soudry 2012). They play an essential role in generating peak bone mass that reduces osteoporosis risk and maintaining a healthy balance of bone anabolism and catabolism (Bonjour et al. 2009; Bergen, Kague, and Hammond 2019). The study of osteoblasts and skeletal development could reveal new therapies and treatments for reduction of osteoporosis rates.

Zebrafish provide an amenable system for studying osteoblast contribution to osteogenesis. Their high fecundity, external fertilization, and rapid initial development makes them an ideal model for investigating the genetic underpinnings of skeletal development. (Tonelli et al. 2020). Furthermore, in zebrafish, these osteoblasts can dedifferentiate into a multipotent progenitor cell pool called a blastema that is capable of completely regenerating the bony structure of their fins (Knopf et al. 2011). The development of additional tools to study osteoblasts in zebrafish will further the understanding of diseases like osteoporosis and barriers to human limb regeneration.

Marker genes have expression profiles that can be used to identify a particular cell type or cell process. These markers can be used to isolate cells for FACS, sequencing, targeted ablation, lineage tracing, or in a number of other experimental methods (Hulett et al. 1969; Liu et al. 2019; Hsu 2015; Abay et al. 2024). Several markers are used to identify osteoblasts as they develop: pre-osteoblasts are marked by *sox9a*/*b*, *runx2a*/*b*; osteoblasts are marked by *sp7* and *runx2a*/*b*; and osteocytes are marked by *col10*, *col1*, *bglap*, and *spp1* (Tonelli et al. 2020). Access to new markers provides insight into different osteoblast subpopulations. For example, the creation of an *sp7:EGFP* transgenic zebrafish line provided an essential tool for the study of zebrafish skeletogenesis and bone regeneration (DeLaurier et al. 2010).

In zebrafish, *slc8a4b* has been identified as a potential osteoblast marker. The gene *slc8a4b* is a member of the calcium/cation antiporter family and produces a protein that is involved in intracellular calcium regulation. Only identified in bony fishes, *slc8a4b* was identified in a phylogenetic analysis of mammalian genes *SLC8A1/2/3* (Marshall et al. 2005). The most similar ortholog, *SLC8A1*, is necessary for proper bone resorption in mice and has genetic variants associated with reduced estimated bone mineral density (Kemp et al. 2017; Albano et al. 2017).

The potential for *slc8a4b* to be used as an osteoblast marker is relatively recent and therefore understudied. First described as an unknown gal4 insertion that marked osteoblasts along scale edges (Iwasaki et al. 2018). A subsequent scRNA-seq analysis of osteoblasts involved in dorsal fin regeneration identified *slc8a4b* as a potential marker for osteoblast progenitors in the blastema (Tang et al. 2022). Shortly after, the gal4 enhancer trap line was shown to be inserted in the *slc8a4b* locus and was used to

mark osteoblasts in the hyomandibular bone (Iwasaki, Kawakami, and Wada 2022). Despite this pre-existing work, the expression patterns and similarity to other osteoblast markers in the developing bone is unknown for *slc8a4b.*

Materials & Methods

Data analysis methods

The single cell RNA seq analysis utilizes a 505 cell subset of the ZSCAPE reference atlas (composed of 1,167 individuals and 1.2 million cells over 19 timepoints (from 18-96 hpf)) produced by Saunders et al. (Saunders et al. 2023).

Management of scRNA seq objects and unsupervised clustering was done using Seurat (Hao et al. 2024). The Saunders data was subset down to the 505 cells identified by Saunders et al. as osteoblasts based on the presence of differentially expressed osteoblast associated genes (*col10a1a, enam, ifitm5, col5a2b, entpd5a, cd81b, si:ch211-106n13.3, slc8a4b, panx3, and tmem119a*) in a cluster produced by principal-component analysis (PCA) (Saunders et al. 2023). To maintain the any transcriptional distinction between proliferating and quiescent osteoblasts, only the difference between the G2M and S phase scores were regressed out (Nestorowa et al. 2016). The dataset was then renormalized and variance stabilized using SCTransform (Choudhary and Satija 2022).

Cell cycle information was taken from the TinyVerse atlas, derived from human orthologues, and hosted by Meeta Mistry ("GitHub - Hbc/Tinyatlas: A Tiny Cell Atlas for Commonly Sequenced Organisms.," n.d.) Seurat-provided cell cycle genes converted to zebrafish orthologs, using babelgene, provided similar results but provided fewer genes found in the Saunders dataset (igor [2021] 2025).

The trajectory analysis was created in a Dynverse wrapper of Slingshot (Street et al. 2018; Saelens et al. 2019). Differentially expressed genes were identified using Seurat. Gene enrichment analyses were performed using the enrichR interface to the Enrichr database for GO and KEGG results (Kuleshov et al. 2016).

ChatGPT was used for coding assistance throughout the project (OpenAI 2025). No large language models were used during writing. The code and custom container used to complete the analysis can be found on Github.

HCR-FISH

Hybridization Chain Reaction Fluorescence in Situ Hybridization (HCR-FISH) to stain for target mRNA expression. HCR-FISH staining followed the standard protocol recommended by molecular instruments with minor changes for optimization ("HCR™ RNA-FISH Protocol for Whole-Mount Zebrafish Embryos and Larvae" 2023).

Images were taken on a Nikon A1 Confocal at 10x and 20x magnification. Laser intensity was set at 5, 5, 5, and 10 for DAPI, B1, B2, and B3 respectively with the gain adjusted by z-stack correction. Images were taken with glavano scanning and a 1.2 AU pinhole. Images were then processed using Fiji to create a maximum intensity z-projection and linearly adjust contrast and brightness for image clarity (Schindelin et al. 2012). All imaged zebrafish were from the wildtype AB line at three days post fertilization (3 dpf or 72 hpf), focused on the opercle and cleithrum of the developing larvae.

Results

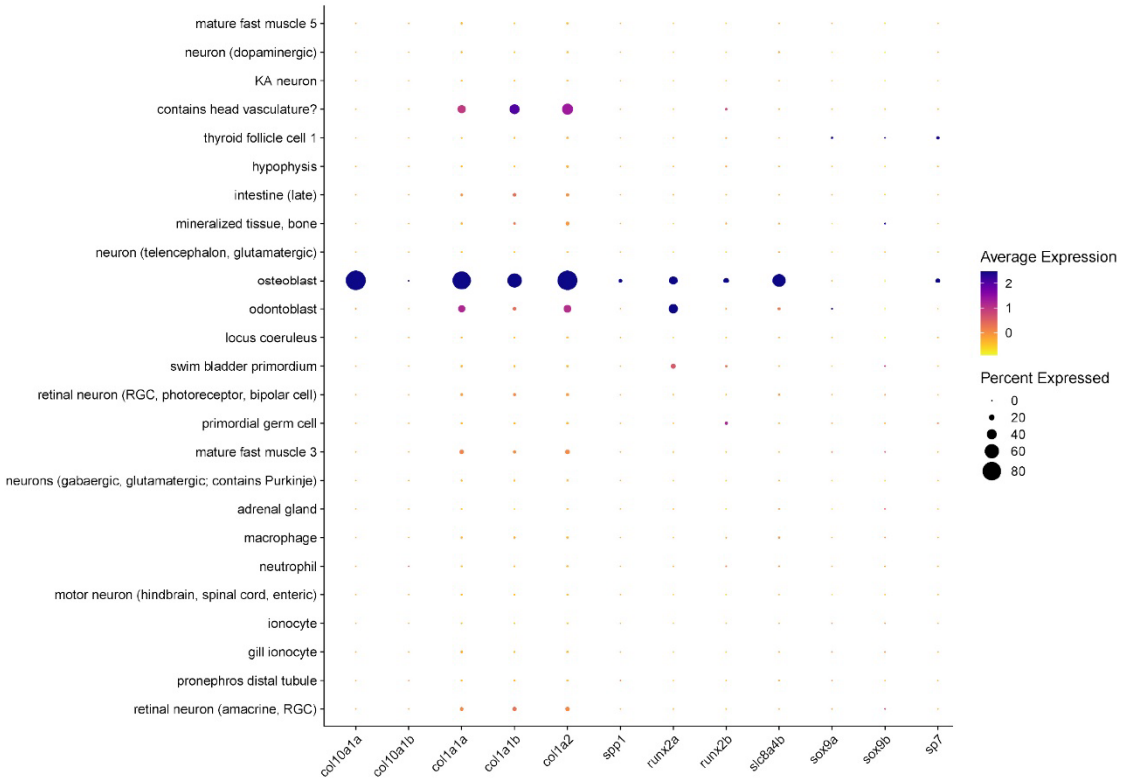

Figure 1 *slc8a4b* is highly and specifically expressed in osteoblasts. A dot plot comparing the expression of various osteoblast markers across a subset of tissue types. Tissue and gene symbols labels are as identified by Saunders et al. Tissues shown are the 25 tissues with the highest percent expression and highest average expression of *slc8a4b*.

High Specificity and Expression of *slc8a4b* within Osteoblasts

The expression of *slc8a4b* is specific to osteoblasts and highly expressed within osteoblasts. Combining the top 25 tissues for average expression of *slc8a4b* and the top 25 tissues for percent expressing *slc8a4b* from the entire Saunders dataset (Figure 1), revealed an *slc8a4b* expression profile that was exceptionally high within and specific to osteoblasts. Osteoblasts had an average *slc8a4b* log-normalized expression of 1.166 and 56.04% of osteoblasts expressing some amount of *slc8a4b.* The next highest average expression and percent expression of *slc8a4b* were in odontoblasts at 0.088 and 7.02% respectively.

Table 1. Counts

Marker Counts within Osteoblast Subset									
Gene Name	*col10a1a*	*col1a2*	*col1a1a*	*col1a1b*	***slc8a4b***	*runx2a*	*runx2b*	*sp7*	*spp1*
Cells Expressing	441	426	394	308	**276**	169	97	72	52

Of selected marker genes, *slc8a4b* captures a greater number of osteoblasts in the Saunders dataset than any of the other non-collagen osteoblast markers (Table 1). Cell counts for cells expressing osteoblast marker genes were compared after binning cells as either expressing (+) the marker gene of interest, i.e. cells with greater than 0.5 log-normalized expression for the marker, or gene non-expressing

(-) cells, i.e. cells with less than or equal to 0.5 log-normalized expression for the marker. Of the 505 osteoblasts in the dataset, 276 cells express some level of *slc8a4b*. The next most commonly expressed osteoblast gene was *runx2a* at 169 cells. One of the most common markers for osteoblasts, *sp7* (*osterix*, an osteoblast-specific transcription factor), was only expressed in 72 cells.

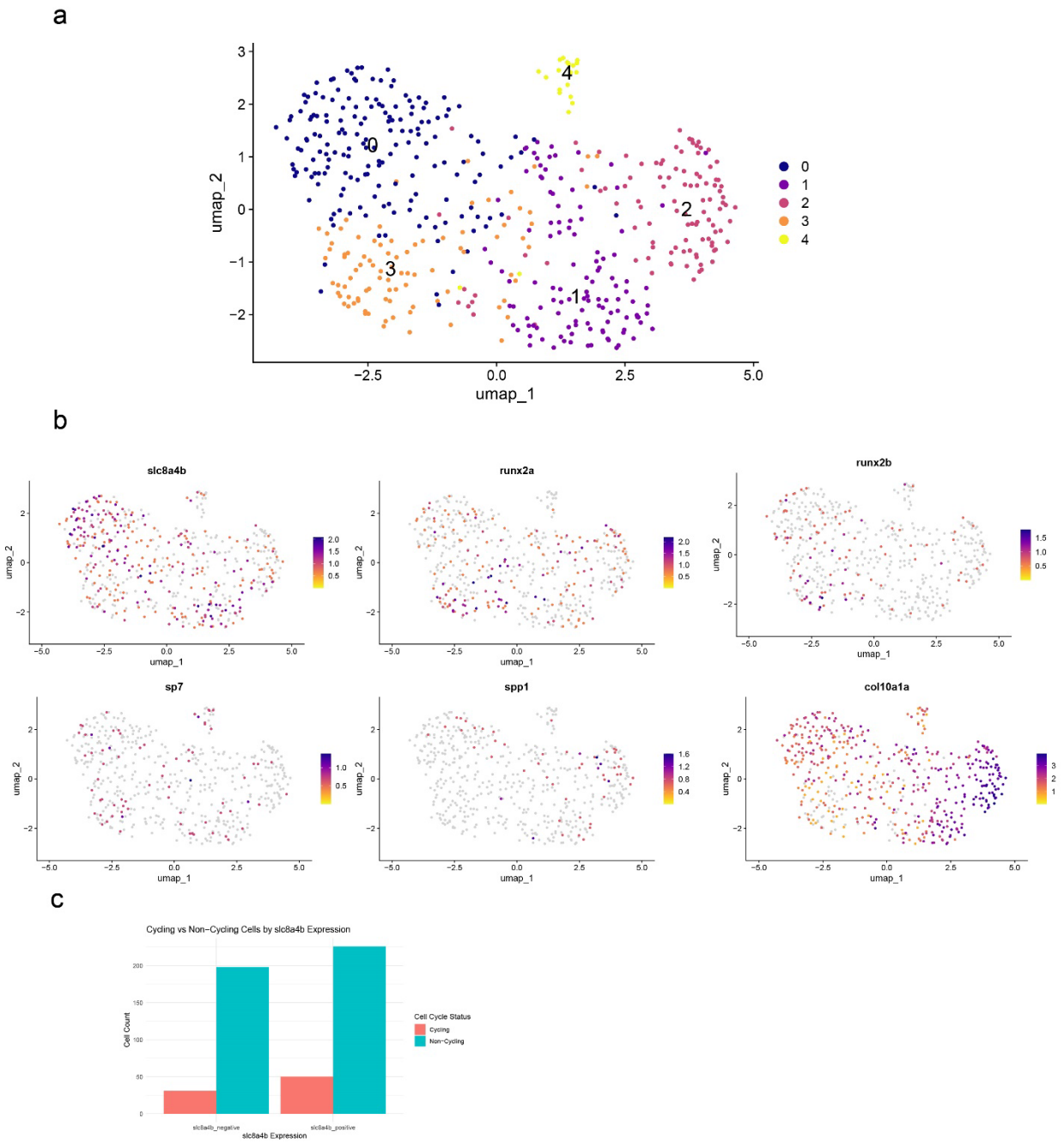

Figure 2 The transcriptional profile of *slc8a4b*+ cells is similar enough to the profiles of other osteoblasts that *slc8a4b* expression is not isolated by unsupervised clustering. (a) A UMAP colored by PCA identities as an example of unsupervised clustering. (b) Feature maps of the UMAP in a colored by expression of: *slc8a4b, runx2a, runx2b, sp7, spp1,* and *col10a1a* (c) Cycling status of *slc8a4b*- and *slc8a4b*+ cells.

Substantial Similarity in Transcriptional Profiles Between Osteoblasts Expressing *slc8a4b* and Osteoblasts Expressing Other Markers

After unsupervised clustering of osteoblasts, *slc8a4b* is found evenly distributed throughout the clusters (Figure 2b). Indicating that the transcriptional differences between *slc8a4b+* cells and *slc8a4b-* cells are too slight for standard principal component analysis to identify. Other osteoblast markers, such as *col10a1a, runx2*, sp7,* and *spp1* are similarly distributed throughout the clusters (Figure 2b).

Cell cycling does not vary significantly with *slc8a4b* expression. After binning cells based on *slc8a4b* expression, Cell cycle scores were compared (Figure 2c). An insignificant chi-square test result supported visual assessment that similar proportions of cells scored as cycling vs noncycling in *slc8a4b+* and *slc8a4b-* cells (Figure 2c).

Table 2. Co-expression

Marker Counts within Osteoblast Subset								
Gene Names	*runx2b*	*col1a1a*	*sp7*	*col10a1a*	*col1a2*	*col1a1b*	*runx2a*	*spp1*
***slc8a4b* Co-expression (%)**	63.90%	57.60%	56.90%	56.70%	54.50%	53.90%	52.10%	46.20%

Additionally, a consistent percentage of cells expressing other osteoblast markers co-expressed *slc8a4b* ($\sigma = 0.048$, $\mu = 55\%$). This was calculated with $(\frac{|s \cap g|100}{|g|})$, where *s* represents *slc8a4b+* cells and *g* represents cells expressing the other gene of interest (Table 1). Apart from *spp1*, the majority of cells expressing an osteoblast marker also express *slc8a4b.*

Differences identified by standard differential gene expression analysis are minor (Figure 3). Cells expressing *slc8a4b* and not *sp7* (*slc8a4b+ sp7-*) have reduced expression of *bzw2*, *gpc5a*, *pik3r1*, *slc6a8*, and *susd6* compared to *slc8a4b- sp7+* cells. These genes have KEGG enrichment scores associated with phosphatidylinositol, VEGF, and ErbB signaling (gene count 1). Similar comparisons showed *slc8a4b- runx2b+* cells enriched for the SCAR complex and actin regulation (gene count 1), *slc8a4b+ and runx2a –* cells enriched for blood vessel morphogenesis and blood vessel development (gene count 3). Comparison *of slc8a4b+* and *slc8a4b-* cells provided enrichment results that indicate *slc8a4b+* cells may have a role in angiogenesis and import into the cell (gene count 2).

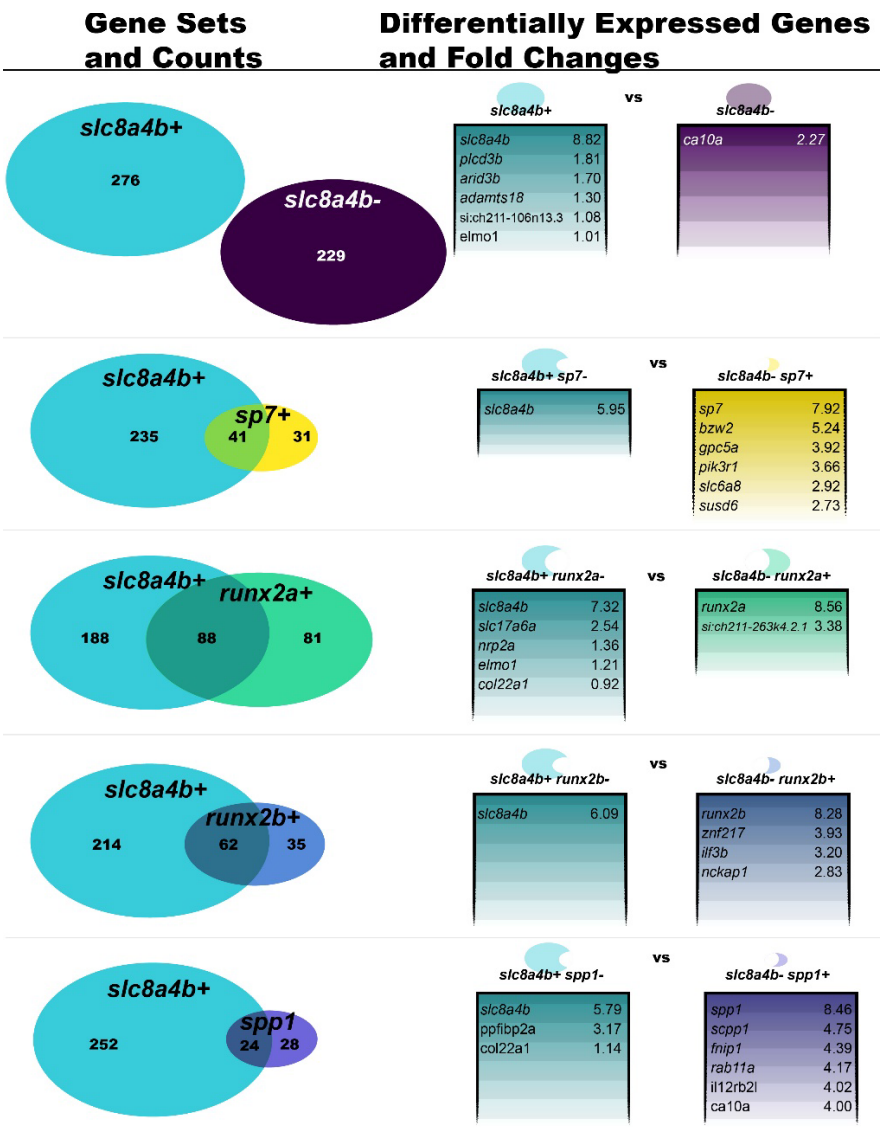

Figure 3 *slc8a4b* expression overlaps with expression of other markers and has few differentially expressed genes. Left are cell counts for osteoblasts expressing *slc8a4b* (*slc8a4b+*), expressing a different gene (*sp7+, runx2a+, runx2b+, spp1+*), expressing both, or not expressing *slc8a4b* (*slc8a4b-)*. On the right are the results of the corresponding differentially expressed markers identified by Seurat::FindMarkers() and filtered for p-value adjusted.

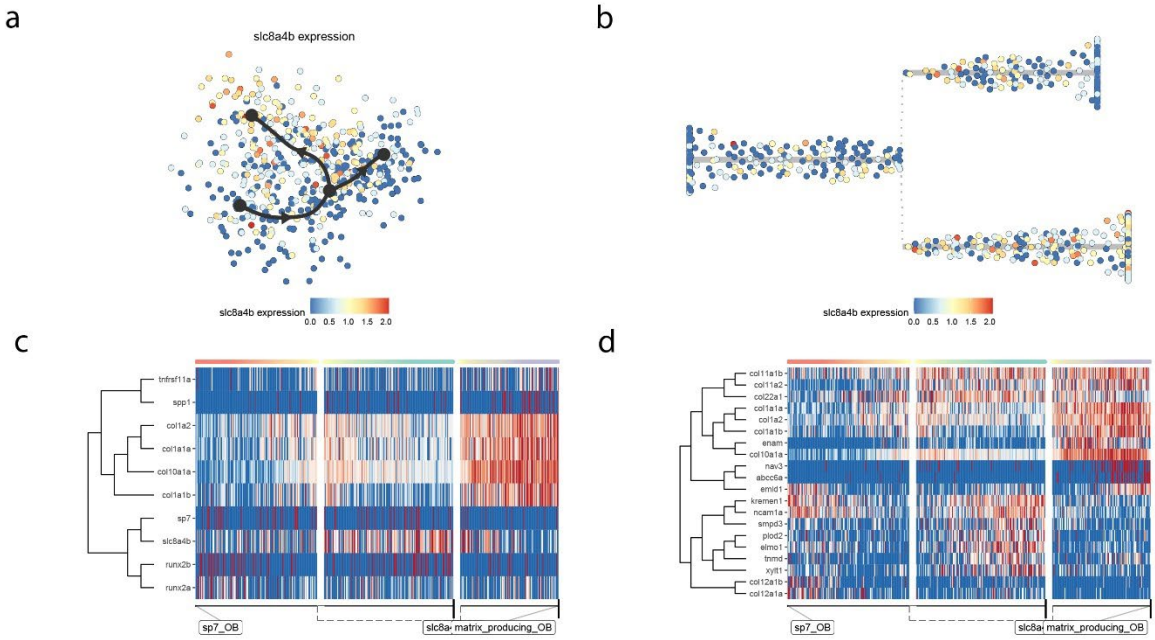

Figure 4 Pseudotime trajectory captures slc8a4b expressing clusters have reduced expression of genes associated with bone matrix production (a) Pseudotime trajectory created by Slingshot in Dynverse mapped over a Seurat produced UMAP. **(b)** The same pseudotime trajectory as in transformed into a dendogram. **(c-d)** a heatmap of key osteoblast gene expression patterns by pseudotime branches and: **(c)** a provided gene list. **(d)** features most important to the pseudotime trajectory calculation.

Expression of *slc8a4b* is Associated with Reduced Expression Matrix Production Genes

An RNA velocity trajectory analysis, conducted within Slingshot, highlighted groups of cells that are associated with both reduced *slc8a4b* expression and reduced expression of genes associated with bone matrix production. This branching expression of *slc8a4b* can be seen in the UMAP (Figure 4a) and more easily seen in the dendogram (Figure 4b).

When provided with common osteoblast markers, the branches with the highest expression of *slc8a4b* have the lowest expression of *tnfrsf11a, spp1, col1a2, col10a1a,* and *col1a1b* (Figure 4c). The pattern of reduced associated with matrix production can still be seen in a more independently produced heatmap that was generated using features identified as important to the construction of the trajectory. These features highlight additional differential gene expression of *enam,* the gene coding for enamlin, and collagen genes, such as *col11a1b, col11a2,* and *col22a1*, that are less expressed within the *slc8a4b* branch (Figure 3d).

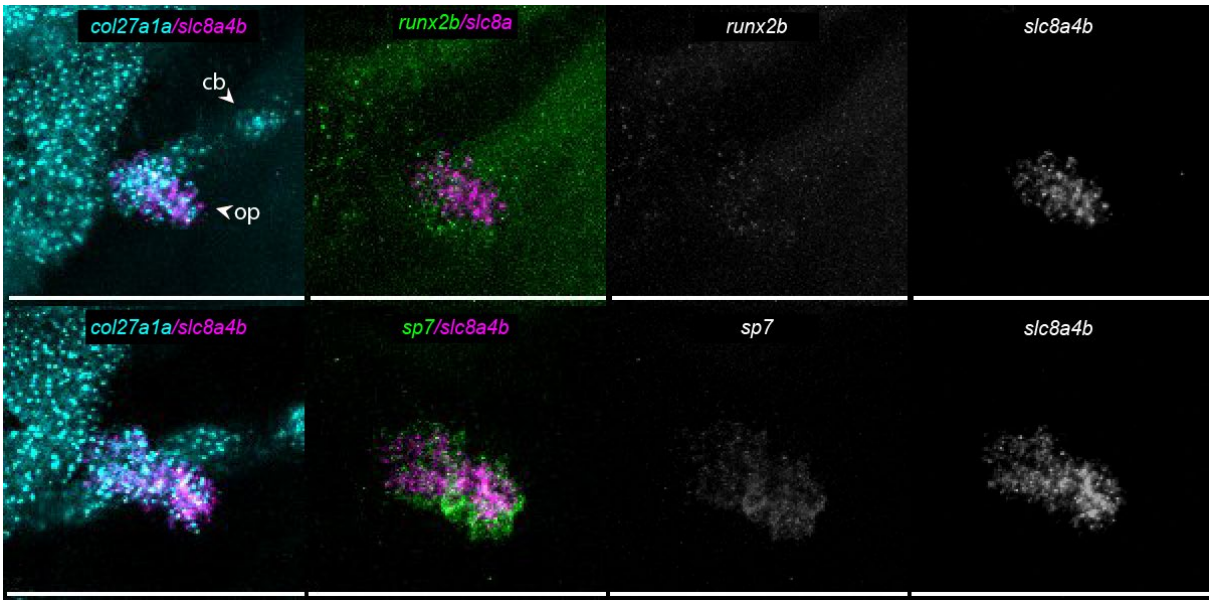

Figure 5 *slc8a4b* is more centralized in the opercle than *runx2b* and *sp7* and more peripheral relative to *col27a1a*. Compared to both *runx2b* and *sp7*, *slc8a4b* is expressed further from the peripheral growth edge and is expressed in a greater number of cells. HCR RNA-FISH was performed using either *col27a1a*, *slc8a4b* (teal), *sp7* or *runx2b* (green), and *slc8a4b* (magenta). These images were taken at 20x magnification. The top left panel labels the opercle (op) and ceratobranchials (cb). All scale bars are 100 μm.

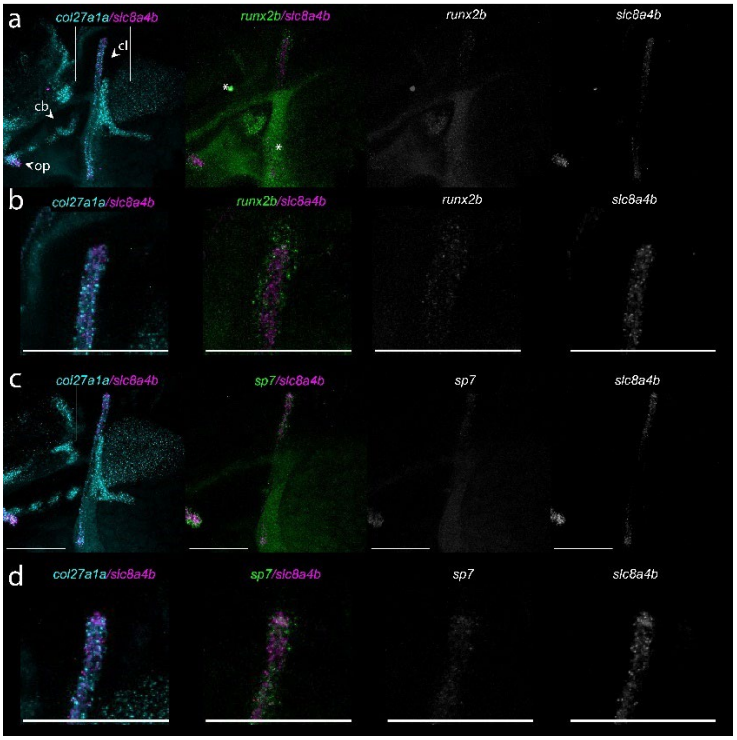

***Figure 6 slc8a4b* has a has more centralized expression in the cleithrum than *runx2b* and *sp7*.** HCR RNA-FISH was performed using either *col27a1a*, *slc8a4b* (teal), *sp7* or *runx2b* (green), and *slc8a4b* (magenta). These images were taken at 20x magnification. Regions of autofluorescence have been marked with a *. Notably, autofluorescent yolk partly obscures the ventral portion of the cleithrum in all channels outside far red. The top left panel labels the opercle (op), ceratobranchials (cb), and cleithrum (cl). All scale bars are 100 μm.

Spatial Expression of *slc8a4b* is Distinct From *runx2b* and *sp7*

HCR images reveal additional spatial expression differences in *slc8a4b* marked cells relative to other osteoblast markers. In the 3dpf opercle, *slc8a4b* is expressed more centrally compared to *sp7* and *runx2b* but has more dorsal/ventral expression relative to *col27a1a,* a marker of developing bone and cartilage. While comparison of expression levels across channels is dubious, there appears to be slightly less *sp7* expression and much less *runx2b* expression than *slc8a4b* expression (Figure 5).

In the 3dpf cleithrum, *slc8a4b* has more centralized expression in the cleithrum than *runx2b*. The expressions of *sp7* and *slc8a4b* appear to share the same domain of expression. However, *slc8a4b* is more broadly expressed within that domain. Relative to *col27a1a*, *slc8a4b* is similarly expressed in the 3dpf cleithrum and is overall more specific to bone tissue (e.g., the cleithrum and opercle) and does not mark cartilage (e.g., the developing ceratobranchials) (Figure 6).

Spatial Expression of *slc8a4b* Closely Overlaps with the Expression of *tnfrsf11a*

The expression pattern of *tnfrsf11a* more closely aligns with *slc8a4b* than *sp7* in the 3dpf opercle. The domains of expression for *sp7* and *slc8a4b* have similar overlap with *tnfrsf11a*. However, *slc8a4b* and *tnfrsf11a* are more similar in their breadth of expression within the domain marked by both than *sp7.*

The co-expression of *slc8a4b* and *tnfrsf11a* has some overlap in the scRNA-seq data as well. Only 144 osteoblasts express *tnfrsf11a* above the previously set 0.5 log-normalized expression threshold. Of these osteoblastic cells, 53% expressing *tnfrsf11a* also express *slc8a4b*.

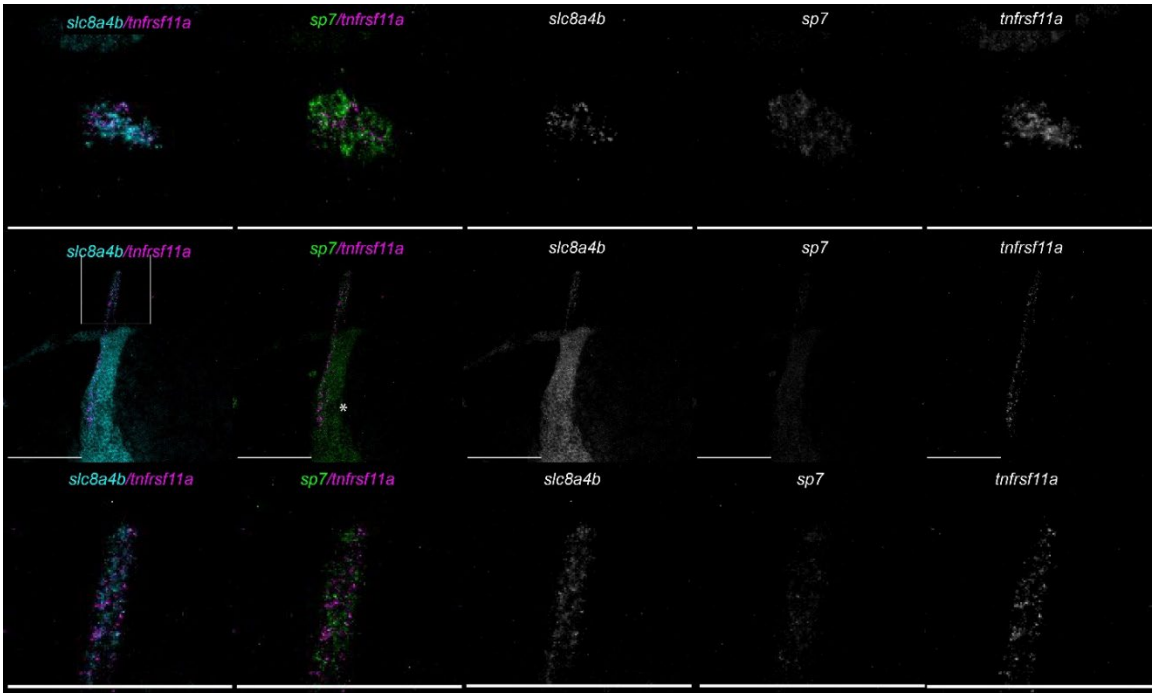

Figure 7 **The expression of *tnfrsf11a* (*RANK*) more closely overlaps with *slc8a4b* than *sp7* in the opercle.** The overlap of *tnfrsf11a* with *slc8a4b* and *sp7* is less clear in the cleithrum. These images were taken at 20x magnification. Regions of autofluorescence have been marked with a *. All scale bars are 100 μm.

Discussion

The scRNA-seq analysis of *slc8a4b* in this study provides a description of *slc8a4b* expression that complements the scRNA-seq work done in Tang et al. Their data focused on osteoblast dedifferentiation and redifferentiation in zebrafish fin regeneration, where *slc8a4b* marked a transcriptionally distinct cluster of non-joint forming osteoblasts in the blastema (Tang et al. 2022). To build on that work, this paper provides the first look at *slc8a4b* expression in osteoblasts during early zebrafish development, where *slc8a4b*+ cells are not as transcriptionally distinct from other osteoblasts with only slight differences in expression.

Despite this similarity, there is some evidence for *slc8a4b*+ osteoblasts to share functions with mature osteoblasts. Previous studies have shown that the 3dpf opercle contains a central intermediate/mature region of bone surrounded by a peripheral early/intermediate region of bone (Li et al. 2009). The centralized expression of *slc8a4b* in the opercle suggested a role in matrix formation, ossification, or another function related to more mature osteoblasts (Figure 5). The pseudotime trajectory analysis identified decreased expression of skeletal matrix synthesizing genes in *slc8a4b*+ cells (Figure 4). Taken together, *slc8a4b*+ cells may be involved in ossification or another function related to more mature osteoblasts but not matrix formation.

Work on the *slc8a4b* loci by Iwasaki et al. indicated *slc8a4b*'s potential use as an osteoblast marker by marking elasmoid scales and the hyomandibular with the DMC13F Gal4 enhancer trap line. The analysis of the scRNA-seq data validates Iwasaki's use of *slc8a4b* as a marker for osteoblasts. The high and specific expression of *slc8a4b* to osteoblasts relative to other tissue types limits off-target expression (Figure 1). While the broad *slc8a4b* expression within osteoblasts that captures a large subset of many other osteoblast markers, that are each associated with different stages of osteoblast development, provides a permissive and less biased selection of osteoblast (Tables 1 & 2, Figures 2 & 3).

The comparison of the Iwasaki's *slc8a4b* enhancer trap line was limited to comparisons of *slc8a4b* with only *sp7* and *pcolcea*, an enzyme involved in collagen synthesis (Iwasaki, Kawakami, and Wada 2022; Iwasaki et al. 2018). The HCR images taken in this study add comparisons of *slc8a4b* and *sp7* in different bones and comparisons of *slc8a4b* with other osteoblast markers, *col27a1a* and *runx2a's* paralog *runx2b.* These images showed that *slc8a4b* expression is more densely clustered within the central region of the 3dpf opercle than *sp7* and *runx2b* and within the central region of the 3dpf cleithrum than *runx2b.* In the cleithrum, *sp7* and *slc8a4b* shared similar domains of expression but *slc8a4b* was more broadly expressed within that domain. Within both bones, *col27a1a* shares a similar expression pattern as *slc8a4b* but is less specific and is also expressed throughout the cartilaginous template of the ceratobranchials (Figures 5-6).

In addition to key osteoblast markers, embryos were stained for *tnfrsf11a* (i.e. RANK) to further demonstrate *slc8a4b* utility in capturing cells poorly captured by other markers. The role of osteoblastic RANK in bone development is an emerging area of research. Previous work has shown RANK is essential for normal osteoblast chemotactic migration during bone remodeling and negatively regulates osteoblastic differentiation from bone marrow mesenchymal stem cells (Golden, Saria, and Hansen 2015; Chen et al. 2018). In zebrafish, our lab identified RANK in osteoblasts during zebrafish development and found RANK to be highly and specifically expressed in zebrafish osteoblasts (Gomez et al. 2024). To

assess *slc8a4b's* use in investigating osteoblastic RANK in developing zebrafish, *tnfrsf11a* expression was compared to *slc8a4b* and an alternative marker*, sp7*. At 3 dpf, the expression pattern of *tnfrsf11a* shares more similarities to *slc8a4b* than *sp7.* Suggesting that *slc8a4b* could be used in future studies of *tnfrsf11a* expression in osteoblasts.

The statistical analysis of the data was limited by the scarcity of osteoblasts in existing zebrafish scRNA-seq datasets. Due to throughput challenges of mRNA extraction in larger specimens, many datasets extract cells only up to 4dpf (Saunders et al. 2023). However, most bone development occurs after 4dpf (Knopf et al. 2011; Tonelli et al. 2020). This challenge is magnified by the dense and mineralized skeletal tissue osteoblasts reside within that further limit successful osteoblast extraction. Creation of datasets with tissue extraction protocols that enrich for osteoblasts or successful integration of multiple datasets may alleviate this challenge (Greenblatt et al. 2019; Johansen and Quon 2019; Lin et al. 2024).

The HCR images in this study focused on the 3dpf opercle and the cleithrum. At 3dpf, both bones are in the beginning stages of their development. Additionally, both the opercle and the cleithrum are formed via intramembranous ossification and are compact cellular bones (Kimmel et al. 2010; Kague et al. 2012; Heubel et al. 2021). Therefore, the HCR images did not compare temporal variation in osteoblast development or variation in bone type.

Future work could include bones that can capture potential variation of *slc8a4b* between additional time points, types of ossification, number of osteocytes in the final bone structure, and new probe combinations. Time points beyond 3dpf would provide a more dynamic view of *slc8a4b's* role in opercle and cleithrum development as well as enabling the study of bones not yet present at 3dpf. Bones such as the ceratohyal, spongy cellular bone formed by type I endochondral ossification; subopercle, acellular compact bone formed by endochondral ossification; and hyomandibular, a tubular bone formed by type II endochondral ossification and perichondral ossification (Weigele and Franz-Odendaal 2016; Tonelli et al. 2020). These bones are expected to express *slc8a4b* based on the expression of *slc8a4b* in hyomandibular and in regenerating acellular dermal bony fin rays shown in previous studies (Tang et al. 2022; Iwasaki, Kawakami, and Wada 2022). Additional study of *slc8a4b* relative to other osteoblast markers in these bones could capture more details about the role of *slc8a4b* in ossification (Weigele and Franz-Odendaal 2016; Siomava et al. 2018). Previous work has identified two osteoblast subpopulations with similar characteristics as observed in HCR RNA-FISH images comparing *sp7* and *slc8a4b* subpopulations: one smaller population on the growth front and another larger population clustered within (Weigele and Franz-Odendaal 2016). Given that Weigele and Franz-Odendaal described a differential expression of *ihha* in these populations, future analysis using an HCR probe for *ihha* could indicate whether these are the same subpopulations they had observed.

Overall, this study provides initial direction for future use and investigation of *slc8a4b* as a marker for zebrafish osteoblasts. Expression of *slc8a4b* in osteoblasts is associated with mature osteoblast functions like ossification, based on the 3dpf opercle results, but not matrix production, based on pseudotrajectory analysis. In the developing 3dpf zebrafish, *slc8a4b* expression is more centralized than *sp7* in the opercle and more centralized than *slc8a4b* in both the opercle and cleithrum. The expression of *slc8a4b* can be used to isolate a large group of osteoblasts that share substantial overlap with other

osteoblast genes of interest. This set of *slc8a4b+* osteoblasts is transcriptionally similar to those captured by some of the most common markers for osteoblasts (such as *runx2** or *sp7)* and includes more osteoblasts than the alternatives. Finally, *slc8a4b* expression more closely captures *tnfrsf11a* expression than *sp7* and *slc8a4b* aiding future studies into RANK signaling within osteoblasts.

Supplemental Table 1: *slc8a4b* Overlap Counts

Gene2	Count: Positive for *slc8a4b* and Positive for Gene2 Expression	Count: Positive for *slc8a4b* and Negative for Gene2 Expression	Count: Negative for *slc8a4b* and Positive for Gene2 Expression	Count: Negative for *slc8a4b* and Negative for Gene2 Expression
runx2b	62	214	35	194
sp7	41	235	31	198
col1a1a	227	49	167	62
col1a2	232	44	194	35
col10a1a	250	26	191	38
runx2a	88	188	81	148
tnfrsf11a	76	200	68	161
spp1	24	252	28	201
col1a1b	166	110	142	87

Supplemental Table 2: Correlation with *slc8a4b*

Gene2	Pearson Correlation of Pseudobulked *slc8a4b*+ and Gene2+ cells	Pearson Correlation of *slc8a4b* and Gene2 Expression
runx2b	0.98329	0.080917
sp7	0.982074	0.017209
col1a1a	0.990188	0.00551
col1a2	0.992437	-0.01231
col10a1a	0.993156	-0.01619
runx2a	0.991448	-0.03087
tnfrsf11a	0.978927	-0.03108
spp1	0.92705	-0.06795
col1a1b	0.982301	-0.12032

Supplemental Table 3: Fractional Overlap

Gene2	Fraction of Intersect Over Both *slc8a4b*+ and Gene2 + cells	Fraction of *slc8a4b*+ Cells Expressing Gene2	Fraction of Gene2+ Cells Expressing *slc8a4b*
runx2b	0.199357	0.224638	0.639175
sp7	0.13355	0.148551	0.569444
col1a1a	0.512415	0.822464	0.576142
col1a2	0.493617	0.84058	0.544601
col10a1a	0.535332	0.905797	0.566893
runx2a	0.246499	0.318841	0.52071
tnfrsf11a	0.22093	0.275362	0.527778
spp1	0.078947	0.086957	0.461538
col1a1b	0.397129	0.601449	0.538961

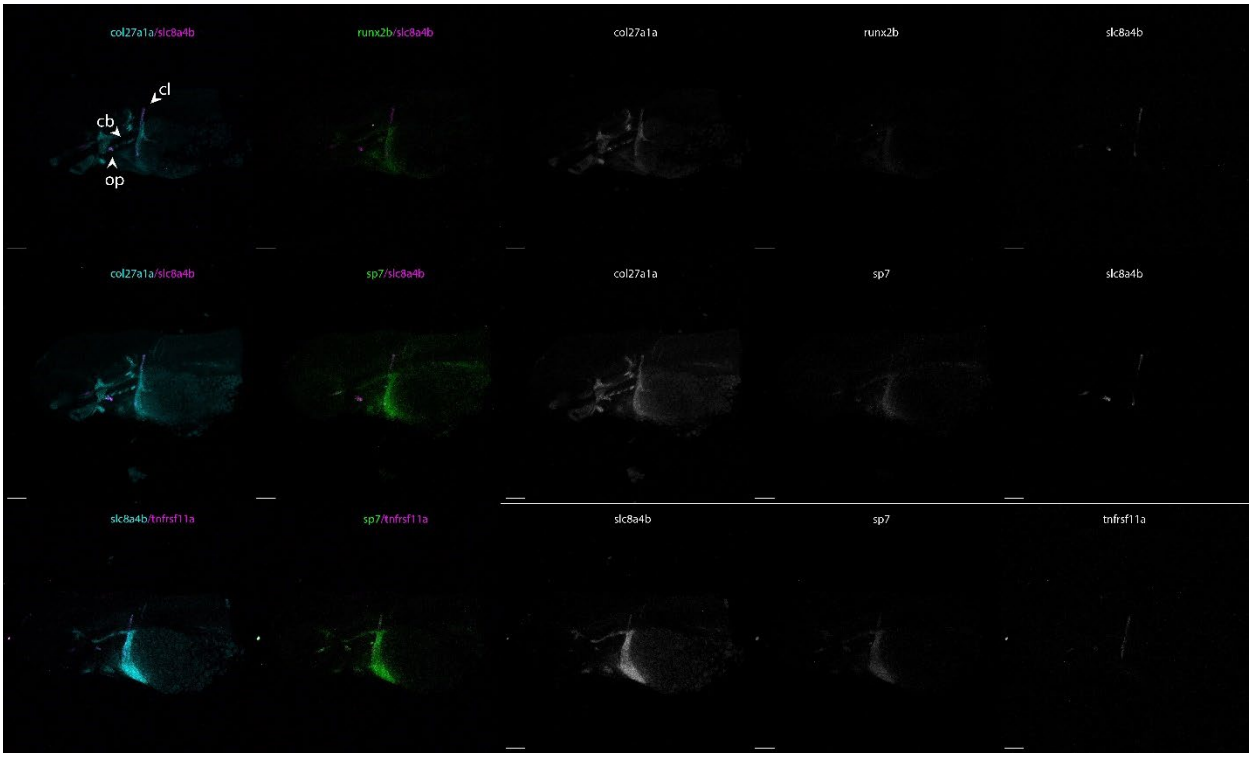

Supplemental Figure 1 *slc8a4b* is expressed in both the opercle and the cleithrum. HCR RNA-FISH was performed using either *col27a1a*, *slc8a4b* (teal), *sp7* or *runx2b* (green), and *slc8a4b* or *tnfrsf11a* (magenta). The top left panel labels the opercle (op), ceratobranchials (cb), and cleithrum (cl). Asterix represents points of autofluorescence. All scale bars are 100 μm.

Bibliography

Abay, Tsion, Robert R. Stickels, Meril T. Takizawa, Benan N. Nalbant, Yu-Hsin Hsieh, Sidney Hwang, Catherine Snopkowski, et al. 2024. “Transcript-Specific Enrichment Enables Profiling Rare Cell States via scRNA-Seq.” *bioRxiv*, March, 2024.03.27.587039. https://doi.org/10.1101/2024.03.27.587039.

Albano, Giuseppe, Silvia Dolder, Mark Siegrist, Annie Mercier-Zuber, Muriel Auberson, Candice Stoudmann, Willy Hofstetter, Olivier Bonny, and Daniel G. Fuster. 2017. “Increased Bone Resorption by Osteoclast-Specific Deletion of the Sodium/Calcium Exchanger Isoform 1 (NCX1).” *Pflügers Archiv - European Journal of Physiology* 469 (2): 225–33. https://doi.org/10.1007/s00424-016-1923-5.

Bergen, Dylan J. M., Erika Kague, and Chrissy L. Hammond. 2019. “Zebrafish as an Emerging Model for Osteoporosis: A Primary Testing Platform for Screening New Osteo-Active Compounds.” *Frontiers in Endocrinology* 10 (January):6. https://doi.org/10.3389/fendo.2019.00006.

Bonjour, Jean-Philippe, Thierry Chevalley, Serge Ferrari, and René Rizzoli. 2009. “The Importance and Relevance of Peak Bone Mass in the Prevalence of Osteoporosis.” *Salud Pública de México* 51. https://doi.org/10.1590/S0036-36342009000700004.

Chen, Xiao, Xin Zhi, Jun Wang, and Jiacan Su. 2018. “RANKL Signaling in Bone Marrow Mesenchymal Stem Cells Negatively Regulates Osteoblastic Bone Formation.” *Bone Research* 6 (1): 34. https://doi.org/10.1038/s41413-018-0035-6.

Choudhary, Saket, and Rahul Satija. 2022. “Comparison and Evaluation of Statistical Error Models for scRNA-Seq.” *Genome Biology* 23 (1): 27. https://doi.org/10.1186/s13059-021-02584-9.

DeLaurier, April, B. Frank Eames, Bernardo Blanco-Sánchez, Gang Peng, Xinjun He, Mary E. Swartz, Bonnie Ullmann, Monte Westerfield, and Charles B. Kimmel. 2010. “Zebrafish Sp7:EGFP: A Transgenic for Studying Otic Vesicle Formation, Skeletogenesis, and Bone Regeneration.” *Genesis (New York, N.Y. : 2000)* 48 (8): 505–11. https://doi.org/10.1002/dvg.20639.

GBD 2019 Fracture Collaborators. 2021. “Global, Regional, and National Burden of Bone Fractures in 204 Countries and Territories, 1990-2019: A Systematic Analysis from the Global Burden of Disease Study 2019.” *The Lancet. Healthy Longevity* 2 (9): e580–92. https://doi.org/10.1016/S2666-7568(21)00172-0.

“GitHub - Hbc/Tinyatlas: A Tiny Cell Atlas for Commonly Sequenced Organisms.” n.d. Accessed March 17, 2025. https://github.com/hbc/tinyatlas.

Golden, Diana, Elizabeth A. Saria, and Marc F. Hansen. 2015. “Regulation of Osteoblast Migration Involving Receptor Activator of Nuclear Factor-Kappa B (RANK) Signaling.” *Journal of Cellular Physiology* 230 (12): 2951–60. https://doi.org/10.1002/jcp.25024.

Gomez, Arianna, Joyce Tang, Priscilla Boatemaa, Edith Gardiner, and Ronald Kwon. 2024. “2024 Annual Meeting of the American Society for Bone and Mineral Research, September 27-30, 2024.” *Journal of Bone and Mineral Research* 39 (Supplement_1): i1–406. https://doi.org/10.1093/jbmr/zjae183.

Greenblatt, Matthew B, Noriaki Ono, Ugur M Ayturk, Shawon Debnath, and Sarfaraz Lalani. 2019. “The Unmixing Problem: A Guide to Applying Single-Cell RNA Sequencing to Bone.” *Journal of Bone and Mineral Research* 34 (7): 1207–19. https://doi.org/10.1002/jbmr.3802.

Hao, Yuhan, Tim Stuart, Madeline H. Kowalski, Saket Choudhary, Paul Hoffman, Austin Hartman, Avi Srivastava, et al. 2024. “Dictionary Learning for Integrative, Multimodal and Scalable Single-Cell Analysis.” *Nature Biotechnology* 42 (2): 293–304. https://doi.org/10.1038/s41587-023-01767-y.

Heubel, Brian P., Carson A. Bredesen, Thomas F. Schilling, and Pierre Le Pabic. 2021. “Endochondral Growth Zone Pattern and Activity in the Zebrafish Pharyngeal Skeleton.” *Developmental Dynamics* 250 (1): 74–87. https://doi.org/10.1002/dvdy.241.
Hsu, Ya-Chieh. 2015. “The Theory and Practice of Lineage Tracing.” *Stem Cells (Dayton, Ohio)* 33 (11): 3197–3204. https://doi.org/10.1002/stem.2123.
Hulett, H. R., W. A. Bonner, Janet Barrett, and Leonard A. Herzenberg. 1969. “Cell Sorting: Automated Separation of Mammalian Cells as a Function of Intracellular Fluorescence.” *Science* 166 (3906): 747–49. https://doi.org/10.1126/science.166.3906.747.
igor. (2021) 2025. “Igordot/Babelgene.” R. https://github.com/igordot/babelgene.
Iwasaki, Miki, Koichi Kawakami, and Hironori Wada. 2022. “Remodeling of the Hyomandibular Skeleton and Facial Nerve Positioning during Embryonic and Postembryonic Development of Teleost Fish.” *Developmental Biology* 489 (September):134–45. https://doi.org/10.1016/j.ydbio.2022.06.009.
Iwasaki, Miki, Junpei Kuroda, Koichi Kawakami, and Hironori Wada. 2018. “Epidermal Regulation of Bone Morphogenesis through the Development and Regeneration of Osteoblasts in the Zebrafish Scale.” *Developmental Biology* 437 (2): 105–19. https://doi.org/10.1016/j.ydbio.2018.03.005.
Johansen, Nelson, and Gerald Quon. 2019. “scAlign: A Tool for Alignment, Integration, and Rare Cell Identification from scRNA-Seq Data.” *Genome Biology* 20 (1): 166. https://doi.org/10.1186/s13059-019-1766-4.
Kague, Erika, Michael Gallagher, Sally Burke, Michael Parsons, Tamara Franz-Odendaal, and Shannon Fisher. 2012. “Skeletogenic Fate of Zebrafish Cranial and Trunk Neural Crest.” *PLOS ONE* 7 (11): e47394. https://doi.org/10.1371/journal.pone.0047394.
Kemp, John P., John A. Morris, Carolina Medina-Gomez, Vincenzo Forgetta, Nicole M. Warrington, Scott E. Youlten, Jie Zheng, et al. 2017. “Identification of 153 New Loci Associated with Heel Bone Mineral Density and Functional Involvement of GPC6 in Osteoporosis.” *Nature Genetics* 49 (10): 1468–75. https://doi.org/10.1038/ng.3949.
Kimmel, Charles B., April DeLaurier, Bonnie Ullmann, John Dowd, and Marcie McFadden. 2010. “Modes of Developmental Outgrowth and Shaping of a Craniofacial Bone in Zebrafish.” *PLoS ONE* 5 (3): e9475. https://doi.org/10.1371/journal.pone.0009475.
Knopf, Franziska, Christina Hammond, Avinash Chekuru, Thomas Kurth, Stefan Hans, Christopher W. Weber, Gina Mahatma, et al. 2011. “Bone Regenerates via Dedifferentiation of Osteoblasts in the Zebrafish Fin.” *Developmental Cell* 20 (5): 713–24. https://doi.org/10.1016/j.devcel.2011.04.014.
Kuleshov, Maxim V., Matthew R. Jones, Andrew D. Rouillard, Nicolas F. Fernandez, Qiaonan Duan, Zichen Wang, Simon Koplev, et al. 2016. “Enrichr: A Comprehensive Gene Set Enrichment Analysis Web Server 2016 Update.” *Nucleic Acids Research* 44 (W1): W90–97. https://doi.org/10.1093/nar/gkw377.
Li, Nan, Katharina Felber, Phil Elks, Peter Croucher, and Henry H. Roehl. 2009. “Tracking Gene Expression during Zebrafish Osteoblast Differentiation.” *Developmental Dynamics* 238 (2): 459–66. https://doi.org/10.1002/dvdy.21838.
Lin, Peng, Yi-Bo Gan, Jian He, Si-En Lin, Jian-Kun Xu, Liang Chang, Li-Ming Zhao, et al. 2024. “Advancing Skeletal Health and Disease Research with Single-Cell RNA Sequencing.” *Military Medical Research* 11 (1): 33. https://doi.org/10.1186/s40779-024-00538-3.
Liu, Fengming, Shen Dai, Dechun Feng, Xiao Peng, Zhongnan Qin, Alison C. Kearns, Wenfei Huang, et al. 2019. “Versatile Cell Ablation Tools and Their Applications to Study Loss of Cell Functions.”

Cellular and Molecular Life Sciences: CMLS 76 (23): 4725–43. https://doi.org/10.1007/s00018-019-03243-w.
Marshall, Christian R., Joanne A. Fox, Stefanie L. Butland, B. F. Francis Ouellette, Fiona S. L. Brinkman, and Glen F. Tibbits. 2005. "Phylogeny of Na+/Ca2+ Exchanger (NCX) Genes from Genomic Data Identifies New Gene Duplications and a New Family Member in Fish Species." *Physiological Genomics* 21 (2): 161–73. https://doi.org/10.1152/physiolgenomics.00286.2004.
Nestorowa, Sonia, Fiona K. Hamey, Blanca Pijuan Sala, Evangelia Diamanti, Mairi Shepherd, Elisa Laurenti, Nicola K. Wilson, David G. Kent, and Berthold Göttgens. 2016. "A Single-Cell Resolution Map of Mouse Hematopoietic Stem and Progenitor Cell Differentiation." *Blood* 128 (8): e20–31. https://doi.org/10.1182/blood-2016-05-716480.
OpenAI. 2025. "ChatGPT." (April Version). 2025. https://chatgpt.com.
Rashki Kemmak, Asma, Aziz Rezapour, Reza Jahangiri, Shima Nikjoo, Hiro Farabi, and Samira Soleimanpour. 2020. "Economic Burden of Osteoporosis in the World: A Systematic Review." *Medical Journal of the Islamic Republic of Iran* 34 (November):154. https://doi.org/10.34171/mjiri.34.154.
Rosenberg, Nahum, Orit Rosenberg, and Michael Soudry. 2012. "Osteoblasts in Bone Physiology—Mini Review." *Rambam Maimonides Medical Journal* 3 (2): e0013. https://doi.org/10.5041/RMMJ.10080.
Saelens, Wouter, Robrecht Cannoodt, Helena Todorov, and Yvan Saeys. 2019. "A Comparison of Single-Cell Trajectory Inference Methods." *Nature Biotechnology* 37 (5): 547–54. https://doi.org/10.1038/s41587-019-0071-9.
Saunders, Lauren M., Sanjay R. Srivatsan, Madeleine Duran, Michael W. Dorrity, Brent Ewing, Tor H. Linbo, Jay Shendure, et al. 2023. "Embryo-Scale Reverse Genetics at Single-Cell Resolution." *Nature* 623 (7988): 782–91. https://doi.org/10.1038/s41586-023-06720-2.
Schindelin, Johannes, Ignacio Arganda-Carreras, Erwin Frise, Verena Kaynig, Mark Longair, Tobias Pietzsch, Stephan Preibisch, et al. 2012. "Fiji: An Open-Source Platform for Biological-Image Analysis." *Nature Methods* 9 (7): 676–82. https://doi.org/10.1038/nmeth.2019.
Siomava, Natalia, Fedor Shkil, Elena Voronezhskaya, and Rui Diogo. 2018. "Development of Zebrafish Paired and Median Fin Musculature: Basis for Comparative, Developmental, and Macroevolutionary Studies." *Scientific Reports* 8 (September):14187. https://doi.org/10.1038/s41598-018-32567-z.
Street, Kelly, Davide Risso, Russell B. Fletcher, Diya Das, John Ngai, Nir Yosef, Elizabeth Purdom, and Sandrine Dudoit. 2018. "Slingshot: Cell Lineage and Pseudotime Inference for Single-Cell Transcriptomics." *BMC Genomics* 19 (1): 477. https://doi.org/10.1186/s12864-018-4772-0.
Tang, W. Joyce, Claire J. Watson, Theresa Olmstead, Christopher H. Allan, and Ronald Y. Kwon. 2022. "Single-Cell Resolution of MET- and EMT-like Programs in Osteoblasts during Zebrafish Fin Regeneration." *iScience* 25 (2): 103784. https://doi.org/10.1016/j.isci.2022.103784.
Tonelli, Francesca, Jan Willem Bek, Roberta Besio, Adelbert De Clercq, Laura Leoni, Phil Salmon, Paul J. Coucke, Andy Willaert, and Antonella Forlino. 2020. "Zebrafish: A Resourceful Vertebrate Model to Investigate Skeletal Disorders." *Frontiers in Endocrinology* 11 (July):489. https://doi.org/10.3389/fendo.2020.00489.
Weigele, Jochen, and Tamara A. Franz-Odendaal. 2016. "Functional Bone Histology of Zebrafish Reveals Two Types of Endochondral Ossification, Different Types of Osteoblast Clusters and a New Bone Type." *Journal of Anatomy* 229 (1): 92–103. https://doi.org/10.1111/joa.12480.